ACS APPLIED MATERIALS & INTERFACES

Research Article

www.acsami.org

Reversible, Self Cross-Linking Nanowires from Thiol-Functionalized Polythiophene Diblock Copolymers

Brenton A. G. Hammer, Marcos A. Reyes-Martinez, Felicia A. Bokel, Feng Liu, Thomas P. Russell, Ryan C. Hayward, Alejandro L. Briseno, and Todd Emrick*

Polymer Science and Engineering Department, University of Massachusetts, Amherst, Massachusetts 01003, United States

Supporting Information

ABSTRACT: Poly(3-hexylthiophene)-*block*-poly(3-(3-thioacetylpropyl) oxymethylthiophene) (P3HT)-*b*-(P3TT) diblock copolymers were synthesized and manipulated by solvent-induced crystallization to afford reversibly cross-linked semiconductor nanowires. To cross-link the nanowires, we deprotected the thioacetate groups to thiols and they subsequently oxidized to disulfides. Cross-linked nanowires maintained their structural integrity in solvents that normally dissolve the polymers. These robust nanowires could be reduced to the fully solvated polymer, representing a novel, reversible cross-linking procedure for functional P3HT-based nanowire fibrils. Field-effect transistor measurements were carried out to determine the charge transport properties of these nanostructures.

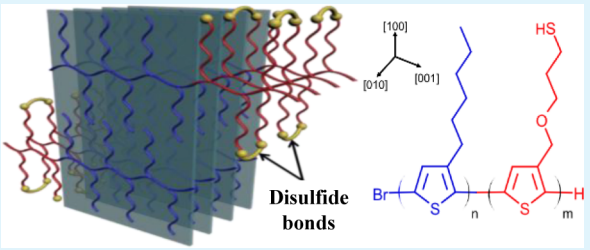

KEYWORDS: *polythiophene, nanowires, self-assembly, reversible cross-linking, organic electronics*

INTRODUCTION

Conjugated polymers are important for organic photovoltaics (OPVs) and other electronic devices based on their low cost, device performance, and good processability.[1−3] One of the key factors in determining OPV performance is the morphology of the electron donor and electron acceptor domains, where an interpenetrating network provides an optimal interface for exciton dissociation and charge transport.[4−8] Poly(3-hexylthiophene) (P3HT) and [6,6]-phenyl-C61-butyric acid methyl ester (PCBM) blends are the most thoroughly characterized donor/acceptor combination in OPVs.[8−10] Attempts to control the morphology of P3HT/PCBM blends include thermal and solvent annealing of thin films, and the deposition of preformed, crystalline nanowires.[10−13] Polythiophene nanowires are formed from a solvent-induced crystallization of the polymer into nanowires, an advantageous architecture since these nanostructures are ideal for hole transport and do not require thermal or solvent annealing following deposition onto a device.[13−17] Blends of nanowires with various electron acceptors have matched OPV device performance of their thin film counterparts, benefiting from improved intermolecular charge transport along the length of the nanowire.[17−19] Jenekhe and co-workers[20] studied poly(3-butyl thiophene) (P3BT) nanowires blended with $PC_{61}BM$ and $PC_{71}BM$, finding that nanowires displayed hole mobilities of 8.0×10^{-3} cm^2 V^{-1} s^{-1} and power conversion efficiency (PCE) value of 3.4%, compared to 1.0×10^{-4} cm^2 V^{-1} s^{-1} and 0.33% for unannealed P3HT/$PC_{61}BM$ thin films. Guillerez and co-workers[21] investigated P3HT fibril and thin film blends with $PC_{61}BM$ in OPVs, and observed a PCE of 3.6% for nanowire based devices, comparable to PCE for annealed P3HT/PCBM blends.

Despite the inherent advantages of conjugated polymer nanowires in OPVs, they are susceptible to macrophase separation over time in blends with PCBM, which significantly decreases device performance.[22,23] P3HT/PCBM blends have been shown to phase separate during extended annealing (≥50 h at 150 °C), reducing PCE to <1.0%.[24,25] Cross-linking the polythiophenes can prevent this by stabilizing the morphology,[26,27] and effective solution methodologies are needed to accomplish this.

Here we describe a P3HT-based diblock copolymer containing pendent thiols that allow cross-linking by oxidation to disulfides. P3HT-*b*-poly(3-(3-thioacetylpropyl)oxymethyl thiophene) (P3TT) diblock copolymers were synthesized, assembled into nanowires, then deprotected and cross-linked oxidatively. A unique quality of disulfide bonds is their ability to be cleaved under reductive conditions, which has been reported for a range of applications such as polymer−drug conjugates, cross-linked micelles, and recyclable polymeric materials.[28−31] This process was applied to our assemblies by reducing the disulfide linkages with dithiothreitol to yield free polymer, demonstrating a new reversible cross-linking process for polythiophene nanowires. Figure 1 depicts the solution assembly of the polymer into nanowires, and cross-linking by disulfide formation.

Received: February 16, 2014
Accepted: April 15, 2014
Published: April 15, 2014

   dx.doi.org/10.1021/am500976w | ACS Appl. Mater. Interfaces 2014, 6, 7705−7711

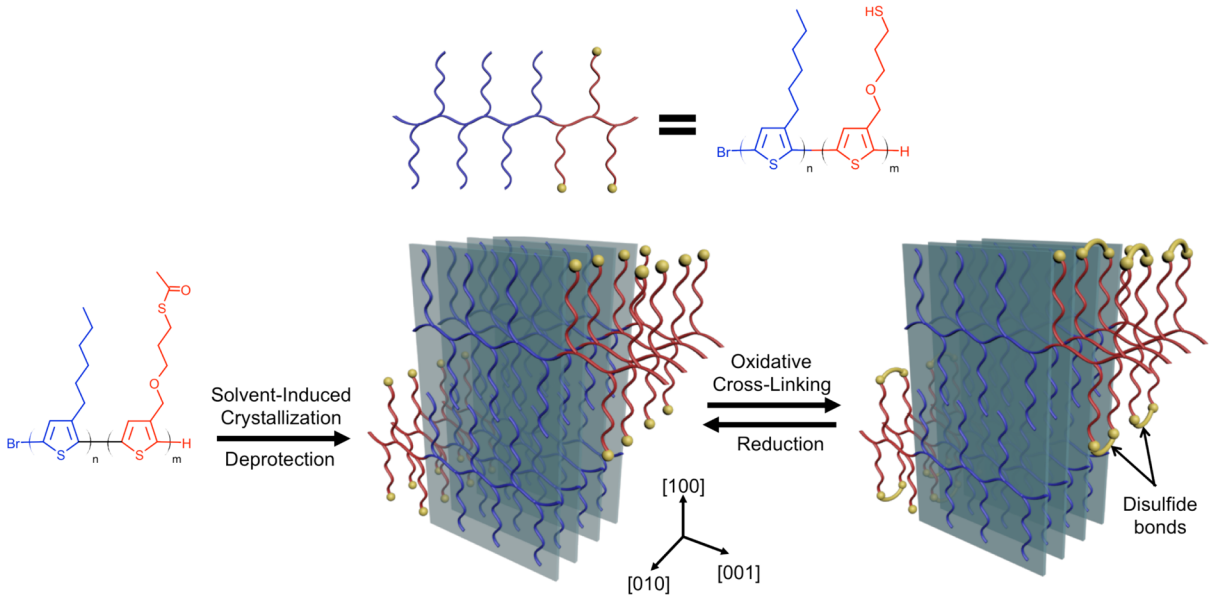

Figure 1. Solution-driven assembly represented by stacked P3HT chains and reversible cross-linking of thiol-functionalized blocks.

EXPERIMENTAL SECTION

Materials. Tetrahydrofuran (THF) was dried over sodium/benzophenone under nitrogen and freshly distilled before use. Chloroform (99%, from Fisher Scientific) was used as received. 3-thiophene methanol (99%, from Aldrich), 3-bromothiophene (97%, from Alfa Aesar), and 1-bromohexane (98%, from Aldrich) were all used as received. N-bromosuccinimide (NBS) (99%, from Acros Organics) was recrystallized in water, and triethyl amine (TEA) was dried over calcium hydride under nitrogen and freshly distilled before use. 3-Bromothiophene (97%, from Alfa Aesar), *tert*-butyl magnesium chloride (2.0 M in diethyl ether, from Aldrich), 3-bromopronol (98%, from Aldrich), and [1,3-bis(diphenylphosphino)propane]-dichloronickel(II) (99%, from Aldrich) were all used as received. All other chemicals were purchased from Aldrich Chemicals and used as received.

Techniques. ^{1}H NMR spectra were recorded on a Brüker-spectrospin 400 using the residual proton resonance of the solvent as the internal standards. Molecular weights of the polymers were estimated by gel permeation chromatography (GPC) with chloroform as the eluent, using polystyrene standard with a refractive index detector. UV/vis absorption spectra were obtained from a Shimadzu 1601 UV spectrometer. Transmission electron microscopy (TEM) images were taken from a JEOL 100CX and 2000FX.

Synthesis. *2,5-Dibromo-3-hexylthiophene (1).* 2,5-Dibromo-3-hexylthiophene was prepared as we previously reported.[32] ^{1}H NMR (400 MHz, CDCl3, δ, ppm): 0.80 (t, 3H), 1.25−1.50 (m, 8H), 2.50 (t, 2H), 6.85 (s, 1H). ^{13}C NMR (400 MHz, $CDCl_3$, δ, ppm): 14.40, 22.88, 29.09, 29.76, 30.00, 31.87, 108.21, 110.60, 131.16, 143.18

2,5-Dibromo-3-thiophenemethanol. 3-Thiophenemethanol (5 g, 4.38×10^{-2} mol) was dissolved in THF (40 mL) in a dried 100 mL round-bottom flask (RBF). The flask was degassed with nitrogen for 15 min before being sealed under a nitrogen atmosphere. NBS (15.59 g, 8.76×10^{-2} mol) was gradually added to the reaction mixture over a 10 min period and the reaction was run at room temperature overnight. The solution was run through a plug of Celite 545 filter powder to remove residual NBS, then the THF was removed via rotary evaporation. The product was dissolved in diethyl ether and then rinsed sequentially with 1 M sodium hydroxide solution and water. The organic layer was concentrated down and the product was run through a silica gel column with an eluent of hexane:ethyl acetate (80:20), collecting the third UV-active spot (relative to the solvent front) seen by thin layer chromatography. The solvent was removed by rotary evaporation to yield the product (10.0 g, 85% yield) as a white solid. ^{1}H NMR (400 MHz, CDCl3, δ, ppm): 4.60 (s, 2H) and 6.70 (s, 1H). ^{13}C NMR (400 MHz, CDCl3, δ, ppm): 58.89, 109.11, 111.43, 130.38, 141.26.

2,5-Dibromo-3-bromomethylthiophene. 2,5-Dibromo-3-thiophenemethanol (5g, 1.84×10^{-2} mol) and dry methylene chloride (100 mL) were added to a 250 mL RBF that was sealed under a nitrogen atmosphere. The solution was placed in an ice bath and stirred for 20 min. Phosphorus tribromide (1.73 mL, 1.84×10^{-2} mol) was added dropwise to the solution over a 15 min period. The reaction was run at room temperature for 5h and then quenched with a 10% sodium bicarbonate solution. The organic solution was passed through a plug of Celite 545, rinsed with water, and then dried over magnesium sulfate. The solution was filtered and dried using rotary evaporation to yield the product (5.8 g, 94% yield) as a light yellow solid. ^{1}H NMR (400 MHz, CDCl3, δ, ppm): 4.80 (s, 2H) and 6.80 (s, 2H). ^{13}C NMR (400 MHz, $CDCl_3$, δ, ppm): 24.18, 111.19, 111.58, 130.28, 137.12.

3-(3-bromopropyl)oxymethylthiophene (2). 2,5-Dibromo-3-bromomethylthiophene (5 g, 1.49×10^{-2} mol) was dissolved in THF (20 mL) in a dried 100 mL RBF. Potassium *tert*-butoxide (1.75 g, 1.56×10^{-2} mol), *tert*-butanol (10 mL), and 3-bromopropanol (2.20 g, 1.58×10^{-2} mol) were added to the solution and the reaction was run at 40 °C for 8 h. The solution was dried by rotary evaporation and run through a silica gel column with a hexane/ethyl acetate (75:25) solvent combination as the eluent. The second UV-active spot (relative to the solvent front) was collected, dried by rotary evaporation to yield the product (3.81 g, 65% yield) as a light yellow liquid. ^{1}H NMR (400 MHz, CDCl3, δ, ppm): 2.20 (m, 2H), 3.50 (t, 2H), 3.60 (t, 2H), 4.55 (s, 2H), and 6.8 (s, 1H). ^{13}C NMR (400 MHz, CDCl3, δ, ppm): 30.56, 32.77, 66.82, 67.82, 110.19, 111.43, 130.81, 139.21.

P3HT-b-P3BPT Diblock Copolymers (3). 2,5-Dibromo-3-hexylthiophene and 2,5-dibromo-3-(3-bromopropyl)oxylmethylthiophene were separately dissolved in THF (20 mL/mg monomer), mixed with their molar equivalent of 2 M *tert*-butyl magnesium chloride, and refluxed for 2 h. The solutions were cooled to room temperature, after which the [1,3-bis(diphenylphosphino)propane]-dichloronickel(II) catalyst was added to the flask with the 2,5-dibromo-3-(3-bromopropyl)oxylmethylthiophene Grignard and reacted for 30 min. An aliquot of the polymer was taken for characterization purposes, and then the 2,5-dibromo-3-hexylthiophene Grignard solution was cannulated into the polymerization flask and reacted for 30 min. The polymerization was quenched with excess methanol (20 mL). The polymer was precipitated in methanol and centrifuged to isolate the polymer from low molecular weight fractions. The polymer was purified by sequential Soxhlet extractions using methanol, hexane, and chloroform, respectively. The chloroform fraction was dried to yield

Scheme 1. Synthesis of P3HT-*b*-P3TT 4 and Thiol-Functionalized Polythiophene 5

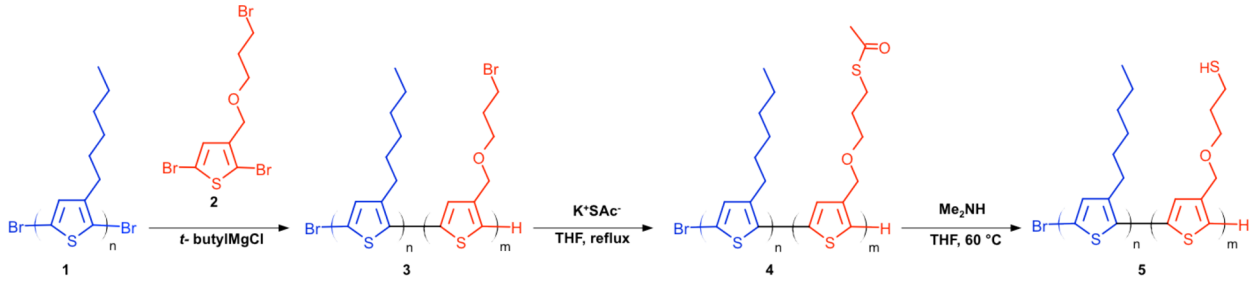

the final polymer as a deep purple solid. Polymerizations were carried out as previously outlined with the following monomer ratios yielding the following polymer samples: 3HT (2.00 g, 6.14 × 10^{-3} mol), 3BPT (0.60 x10^{-1} g, 1.53 × 10^{-3} mol) mixed with their molar equivalents of the Grignard reagent, and Ni(dppp)Cl_2 (6.40 × 10^{-2} g, 1.18 × 10^{-4} mol) yielded (65% yield, 3:1 weight ratio, M_n =11 300 g/mol, PDI = 1.35). 3HT (2.00 g, 6.13 × 10^{-3} mol), 3BPT (4.50 × 10^{-1} g, 1.06 × 10^{-3} mol), and Ni(dppp)Cl_2 (4.43 × 10^{-2}, 8.17 × 10^{-5} mol) yielded (70% yield, 4:1 weight ratio, M_n = 15 100 g/mol, PDI = 1.25). ^{1}H NMR (400 MHz, CDCl3, δ, ppm): P3HT- 0.85 (t, 3H), 1.25−1.70 (m, 8H), 2.70 (t, 2H), 7.00 (s, 1H). ^{13}C NMR (400 MHz, $CDCl_3$, δ, ppm): 14.32, 22.84, 29.45, 29.65, 30.69, 31.88, 128.77, 130.64, 133.85, 140.05. P3BPT 2.20 (m, 2H), 3.50 (m, 3H), 3.70 (m, 1H), 4.55 (m, 1H), 4.65 (m, 1H), 7.00 (s, 1H). ^{13}C NMR (400 MHz, $CDCl_3$, δ, ppm): P3BPT 30.55, 32.77, 66.81, 67.82, 129.32, 131.01, 133.69, 137.48. FT-IR (cm^{-1}): 3000, 2967, 2829, 1504, 1164, 876.

*P3HT-b-poly(3-(3-thioacetetatepropyloxylmethyl) thiophene) (P3TT) (**4**).* P3HT-*b*-P3BPT (5.00 × 10^{-1} g, 3.30/4.42 × 10^{-5} mol) was dissolved in THF (20 mL) in a 100 mL RBF. Potassium thioacetate (1.5/2.0 × 10^{-1} g, 1.32/1.77 × 10^{-3} mol) was added, and the solution was refluxed for 4 h. The solution was run through a plug of Celite 545 filter aid and dried by rotary evaporation. The polymer was dried down to yield the final product as a deep purple solid (4.45 × 10^{-1} g, 89% yield). M_n = 11 100/15 00 g/mol, PDI = 1.40/1.30 ^{1}H NMR (400 MHz, CDCl3, δ, ppm): P3TT 1.90 (m, 2H), 2.35 (s, 3H), 3.00 (m, 2H), 3.50 (m, 1H), 3.60 (m, 1H), 4.45 (m, 1H), 4.60 (m, 1H) 7.00 (s, 1H). ^{13}C NMR (400 MHz, $CDCl_3$, δ, ppm): P3TT 29.79, 30.61, 33.01, 66.99, 67.54, 129.40, 131.10, 133.57, 137.48, 185.25. FT-IR (cm^{-1}): 2989, 2972, 2907, 1757, 1520, 1332, 1283, 1138, 1028, 791.

*P3HT-b-poly(3-thiolpropyloxylmethylthiophene) (P3ST) (**5**).* Polymer **5** (2.50 x10^{-1}g, 1.66/2.17 × 10^{-5} mol) was dissolved in THF (20 mL) that was degassed by three freeze−pump−thaw-cycles, 1 M dimethyl amine (6.65/8.68 × 10^{-1} mL, 6.65/8.68 × 10^{-4} mol) was added and the reaction was run at 60 °C for 2 h. The reaction was dried by rotary evaporation. The resulting polymer underwent sequential Soxhlet extractions using methanol and chloroform, respectively. The chloroform fraction was dried by rotary evaporation to yield the desired polymer as a deep purple solid (1.95 × 10^{-1} g, 85% yield). P3ST ^{1}H NMR (400 MHz, CDCl3, δ, ppm): 2.00 (m, 2H), 2.55 (m, 2H), 3.55 (m, 1H), 3.65 (m, 1H), 4.50 (m, 1H), 4.60 (m, 1H), 7.00 (s, 1H). ^{13}C NMR (400 MHz, $CDCl_3$, δ, ppm): 29.55, 30.71, 66.85, 67.81, 129.39, 131.11, 133.60, 137. 49. FT-IR (cm^{-1}): 2966, 2931, 2912, 2470, 1472, 1264, 1105, 1029, 824.

Solution Preparation of Fibrils. Fibrils were formed under nitrogen atmosphere while protected from light. To induce aggregation, we added a respective amount of dichloromethane (7 mL) to P3HT-*b*-P3TT (10 mg/mL) in chloroform.

Assembly Cross-Linking Procedure. P3HT-*b*-P3TT (10 mg, 6.6/9.0 × 10^{-7} mol) was dissolved in $CHCl_3$ (1 mL) in a 20 mL vial. CH_2Cl_2 (7 mL) was added to the solution and fibril formation was allowed to proceed overnight. Cross-linked fibrils were achieved with the following concentrations of polymer functional groups:dimethyl amine relative ratios in 1:7/11 $CHCl_3$:CH_2Cl_2: 3 mM:50 mM. The solutions were mixed for 8 h at room temperature to achieve sufficient cross-linking. Adding iron(III) chloride as an oxidizing agent (5 mM) accelerated the cross-linking process to 1 h. Once cross-linking was achieved the solutions were dried by rotary evaporation, suspended in THF, and isolated by centrifugation to achieve stable nanowires (7.8 mg, 80% yield) as a deep purple solid. FT-IR (cm^{-1}): 2981, 2976, 2889, 2502, 1483, 1223, 1107, 1029, 786.

Reduction of Cross-Linked Fibrils. Cross-linked fibrils (20 mg) were suspended in THF (5 mL) that underwent three freeze−pump−thaw cycles. Dithiothreitol (10 mg) was added to the solution and heated at 60 °C for 1 h. The mixture was passed through a plug of Celite 545 filter aid and dried by rotary evaporation to yield the product as a deep purple solid (16 mg). P3ST ^{1}H NMR (400 MHz, CDCl3, δ, ppm): 2.00 (m, 2H), 2.55 (m, 2H), 3.55 (m, 1H), 3.65 (m, 1H), 4.50 (m, 1H), 4.60 (m, 1H), 7.00 (s, 1H). ^{13}C NMR (400 MHz, $CDCl_3$, δ, ppm): 29.55, 30.71, 66.85, 67.81, 129.39, 131.11, 133.60, 137. 49.

TEM for the study of self-assembled structures of P3HT-*b*-P3TT assemblies in chloroform/dichloromethane solvent mixtures, and in chloroform for cross-linked assemblies (1 mg/mL) were drop cast on a carbon-coated copper grid and allowed the solution to evaporate under ambient conditions. UV−vis spectroscopy was carried out with 0.1 mM solutions of sample.

GIXD Characterization. The experimental setup and sample cell were designed for studying the bulk samples. An X-ray beam impinged onto the sample directly. The sample thickness is less than a millimeter. The wavelength of X-rays used was 1.240 Å, and the scattered intensity was detected by using two-dimensional Pilatus detector with image sizes of 981 × 1043 pixels (Pixel size 172 × 172 mm^2). The scattering image data was processed by using Nika package.

Field-Effect Mobility Studies. Field-effect transistors were fabricated using a bottom gate/bottom contact configuration. Heavily doped silicon functioned as bottom gate with a 300 nm thermally grown silicon dioxide as gate insulator. Ti/Au interdigitated source and drain electrodes (400 μm channel width, 600 μm channel length) were deposited on the surface of silicon dioxide using photolithography. Substrates were cleaned by rinsing with acetone and isopropyl alcohol. All devices were UV-ozone treated for 20 min. Prior to casting the active layers, the surface was treated with hexamethyldisilazane (HMDS) by spin coating at 2,000 rpm. P3HT-*b*-P3AmT fibril solutions (1.25 mg/mL) were spun cast at 2000 rpm yielding films ~130 ± 23 nm thick. Cross-linked P3HT-*b*-P3AmT fibrils were spun cast at 4000 rpm yielding films ~116 ± 93 nm thick. All spin coating steps were performed in a N_2 atmosphere. Field-effect mobility (μ) was extracted from operation in the saturation regime using the standard equation: $I_D = \mu(W/2L)C_i(V_G - V_T)^2$, where I_D is drain current, μ is field-effect mobility, W is the channel width, L is the channel length, C_i is he capacitance of the gate insulator per unit area (10nF/cm^2), V_G is the gate voltage, and V_T is the threshold voltage. Field-effect charge mobilities were averaged over 6 samples from 3 different fibril batches.

RESULTS AND DISCUSSION

Scheme 1 shows the synthesis of P3HT-*b*-P3TT (**4**) and subsequent deprotection to thiol-functionalized diblock copolymer **5**. The P3HT block was synthesized by Grignard metathesis (GRIM) polymerization, and chain-extended with

2,5-dibromo-3-(3-bromopropyl)oxymethylthiophene to yield diblock copolymer **3**.[32] Reaction of brominated diblock **3** (2.21 mM) with potassium thioacetate (88.5 mM) in THF at reflux for 4 h gave P3HT-*b*-P3TT. ^{1}H NMR spectroscopy showed a methylene signal adjacent to the thioacetate at 3.00 ppm, with >95% conversion from bromide to thioacetate. Fourier transform infrared spectroscopy (FT-IR) of P3HT-*b*-P3TT revealed a carbonyl signal at 1757 cm^{-1} associated with the thioacetate functionality.

The relative block ratios in **4** (molar monomer equivalent) were determined by ^{1}H NMR spectroscopy, comparing the methylene protons adjacent to the thiophene ring of P3HT (2.70 ppm) and P3TT (4.55 ppm). The P3HT block was the larger of the two blocks (75−80 mol %) to promote nanowire formation. Table 1 gives molecular weight data for P3HT-*b*-P3BPT and P3HT-*b*-P3ST, ranging from 11 to 15 kDa with PDI values of 1.25−1.50.

Table 1. Molecular weights of P3HT-b-P3BPT, P3HT-b-P3TT, and P3HT-b-P3ST diblock copolymers

entry	polymer	$M_{n(Theor.)}$ (g/mol)[a]	$M_{n(Exp.)}$ (g/mol)[b]	PDI[b]	P3HT:P3BPT molar ratios[c]
1	P3HT-*b*-P3BPT	12 000	11 320	1.35	3:1
2	P3HT-*b*-P3TT		11 150	1.40	3.1:1
3	P3HT-*b*-P3ST		10 980	1.50	2.8:1
4	P3HT-*b*-P3BPT	16 000	15 140	1.25	4:1
5	P3HT-*b*-P3TT		15 040	1.30	3.9:1
6	P3HT-*b*-P3ST		14 770	1.30	3.9:1

[a]Calculated from monomer-to-catalyst ratio. [b]Estimated by GPC against PS standards. [c]Determined by ^{1}H NMR spectroscopy.

Figure 1 depicts the solution assembly of the polymer into nanowires, and cross-linking by disulfide formation. Solvent-induced crystallization of P3HT-*b*-P3TT was achieved by dissolving 10 mg of polymer in 1 mL of good solvent ($CHCl_3$), then diluting the solution with 7 mL of a less favorable solvent (CH_2Cl_2). As shown in Figure 2, ultraviolet−visible (UV−vis)

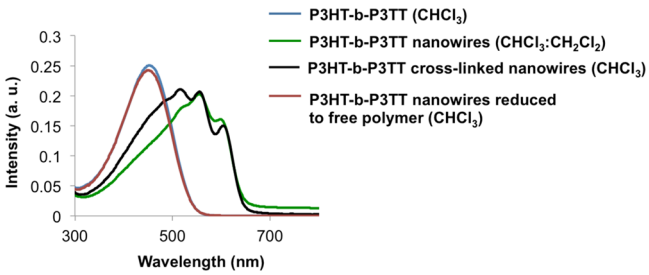

Figure 2. UV−vis spectra. P3HT-*b*-P3TT solvated ($CHCl_3$), nanowires (1:7 $CHCl_3$:CH_2Cl_2), cross-linked nanowires ($CHCl_3$), reduction to solvated polymer ($CHCl_3$).

spectroscopy was used to monitor the transition from solvated polymer in $CHCl_3$ (461 nm) to nanowires having characteristic vibronic absorption bands at 532, 563, and 607 nm, associated with $\pi-\pi$ stacking of the polythiophene chains. Importantly, the presence of the thioacetates of **4** did not disrupt nanowire formation that is typical of P3**R**T structures (when **R** = alkyl).

In nanowire form, P3HT-*b*-P3TT (3.0 mM) was deprotected with dimethylamine (50 mM) in $CHCl_3$:CH_2Cl_2 (1:7), and in the presence of oxygen the resulting thiols oxidized to form disulfide linkages that covalently cross-link the nanowires. FT-IR spectroscopy showed a significant decrease in the carbonyl signal (1757 cm^{-1}) because of the absence of the thioacetates (see Figure S1 in the Supporting Information). Cross-linking was considered complete when the nanowires oriented at the air/solvent interface (see Figure S2 in the Supporting Information), and confirmed when an aliquot (0.1 mL) was diluted in a good solvent for P3HT (2.5 mL of $CHCl_3$), yet maintained nanowire vibronic absorption bands (532, 563, and 607 nm) in the UV−vis spectrum (Figure 2). P3HT-*b*-P3TT nanowires cross-linked oxidatively in 8 h by simply leaving the polymer solution open to air. Moreover, cross-linking was accelerated significantly by the presence of a catalytic amount of $FeCl_3$ (5 mM) in the solution. After either cross-linking method, the resultant nanowires were diluted in THF, isolated by centrifugation to remove free polymer, and suspended in $CHCl_3$.

Transmission electron microscopy (TEM) characterization (Figure 3A) showed nanowires with widths ∼15−25 nm and

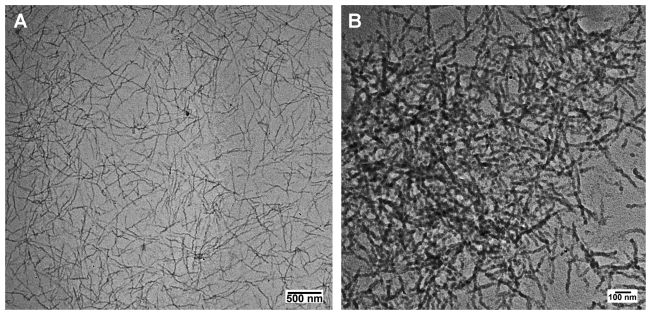

Figure 3. TEM images of (A) P3HT-*b*-P3TT nanowires (drop cast from 1:7 $CHCl_3$:CH_2Cl_2); and (B) cross-linked P3HT-*b*-P3ST nanowires (≥6 mM).

lengths ∼0.4−3 μm. TEM images of the cross-linked nanowires (drop cast from a 1.5 mg/mL $CHCl_3$ solution) showed bundles with individual structures having widths ∼20−25 nm and lengths between ∼0.2−1 μm (Figure 3B). Crucial to the success of this design, the cross-linked nanowires showed stability to a variety of solvents ($CHCl_3$, chlorobenzene, and toluene) that readily dissolve uncross-linked nanowires, and moreover stability at elevated temperatures (≥150 °C), as seen in Figure S3 in the Supporting Information.

A unique aspect of this cross-linking mechanism is its reversibility, a characteristic not described previously for such nanowires in solution or the solid state. The disulfides were reduced in the presence of dithiothreitol (DTT, 2 mg/mL, 60 °C, 1 h) to recover the original solvated polymer. UV−vis spectroscopy (Figure 2) in $CHCl_3$ showed a shift in absorption intensity from the vibronic absorption bands of the cross-linked nanowires back to solvated polymer.

To probe the effect of cross-linking on nanowire structure, P3HT-*b*-P3TT nanowires before and after cross-linking were characterized by solid state grazing incidence wide-angle X-ray diffraction (GI-WAXD). The *d*-spacing between polymer chains in the (100) and (010) planes was calculated as $d = 2\pi/q$ (Å), and the scattering profiles are shown in Figure 4. P3HT-*b*-P3TT showed reflections at 0.376 Å^{-1} in the (100) direction and 1.62 Å^{-1} in the (010) direction. From these

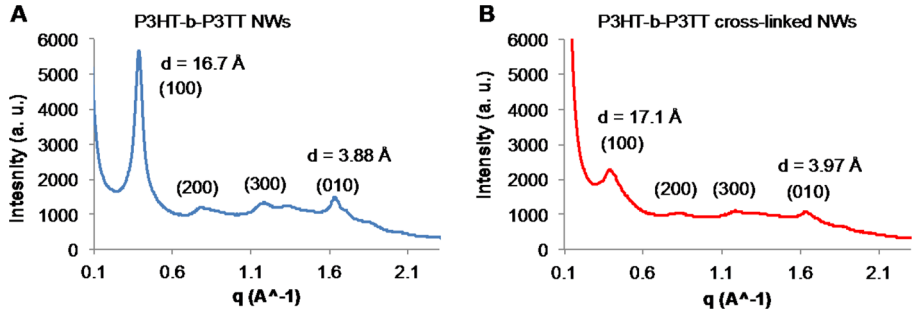

Figure 4. GI-WAXD diffraction profiles for (A) P3HT-*b*-P3TT nanowires and (B) P3HT-*b*-P3TT/ST cross-linked nanowires.

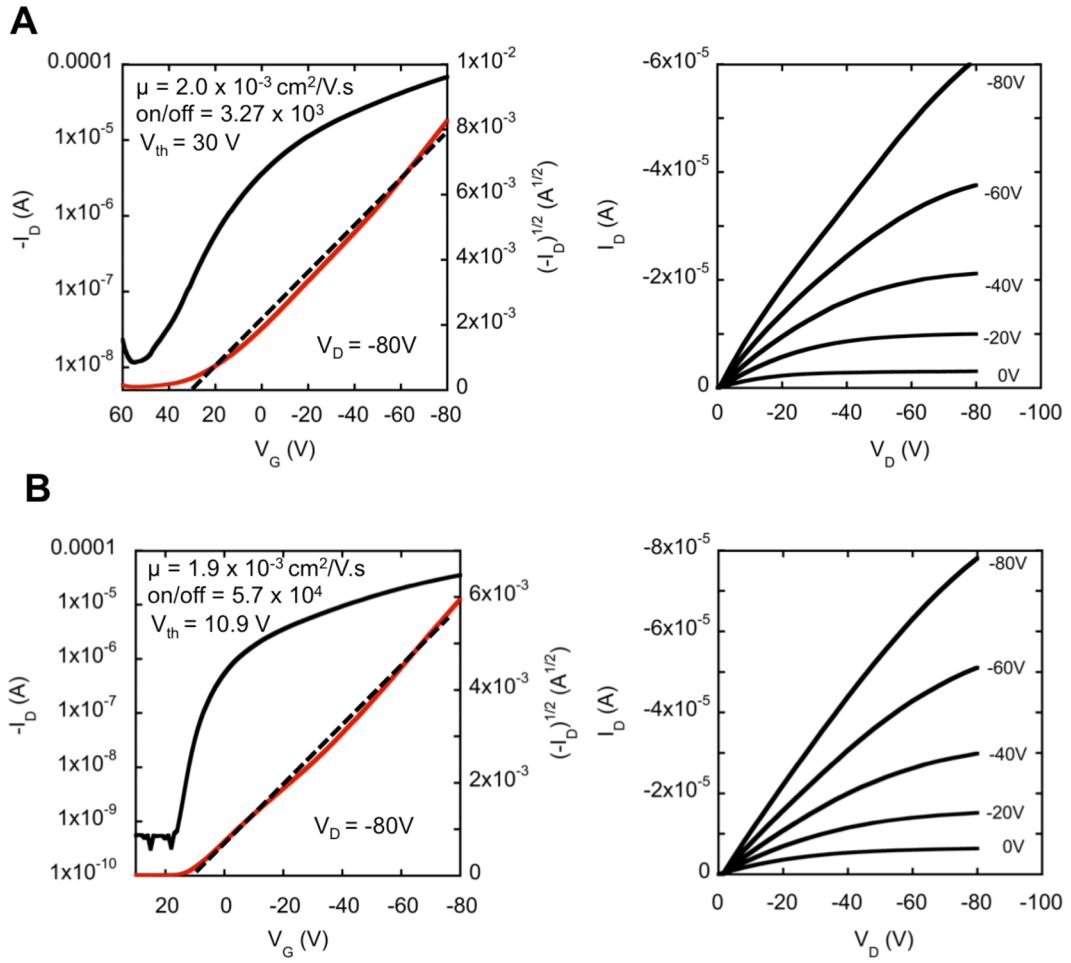

Figure 5. Representative field-effect transistor characteristics. (A) Transfer and output characteristics for P3HT-*b*-P3TT nanowires. (B) Transfer and output curves corresponding to P3HT-*b*-P3TT cross-linked nanowires.

values, the polymer chain spacing in the (100) plane was calculated as 16.7 Å, and in the (010) plane as 3.88 Å, in close agreement with literature values for P3HT nanowires.[33] Cross-linked P3HT-*b*-P3TT nanowires showed reflections at 0.367 $Å^{-1}$ ((100) plane) and 1.58 $Å^{-1}$ ((010) plane), which correlate to a (100) spacing of 17.1 Å and (010) spacing of 3.97 Å. The slightly larger spacings after cross-linking ((100) (0.4 Å) and (010) (0.09 Å)) show that only a marginal change is imposed on the polymer chain packing as a result of cross-linking, and suggest that mobilities should not be altered significantly.

Field-effect hole mobilities were characterized using bottom-gate, bottom-contact transistor structures with interdigitated source and drain electrodes. P3HT-*b*-P3TT nanowire solutions (1.25 mg/mL) were spun cast at 2000 rpm, yielding ~140 nm films as measured by contact profilometry. Representative transfer and output characteristics for P3HT-*b*-P3TT nanowires transistors before and after cross-linking are shown in Figure 5. P3HT-*b*-P3TT uncross-linked nanowires displayed average hole mobilities $\mu_{eff} \approx 2.0 \times 10^{-3} \pm 4.4 \times 10^{-4}$ cm^2 V^{-1} s^{-1}, average threshold voltage $V_{th} \sim 30.6 \pm 2.0$ V and average current on/off ratios of approximately 4×10^3 (Figure 5A). After oxidative cross-linking, the nanowires showed $\mu_{eff} \approx 1.98 \times 10^{-3} \pm 4.33 \times 10^{-5}$ cm^2 V^{-1} s^{-1}, $V_{th} \approx 11.2 \pm 0.2$ V and average current on/off ratios of approximately 3×10^4 (Figure 5B). These measurements indicate that the cross-linking process does not significantly alter charge carrier mobility.

dx.doi.org/10.1021/am500976w | ACS Appl. Mater. Interfaces 2014, 6, 7705−7711

Interestingly, threshold voltage is improved by approximately a factor of 3 and current on/off ratio is an order of magnitude higher. The measured mobilities are in agreement with the average mobilities for P3HT homopolymer (1×10^{-2} to 1×10^{-3} cm^2 V^{-1} s^{-1}).[33]

CONCLUSIONS

In summary, we have described the synthesis of thiol-containing polythiophene diblock copolymers, their solvent-induced crystallization into nanowires, and oxidative cross-linking. This novel self-assembling system does not require additives for cross-linking, giving nanowires that are stable in a variety of solvents with little perturbation to their crystal structure and field-effect mobility values after cross-linking. The cross-linking was shown to be stable to both solvents and elevated temperatures, yet clearly reversible by reduction with DTT. This represents a novel method for self-cross-linking of conjugated polymer nanowires, yielding robust assemblies that maintain their crystal structure and charge transport characteristics.

ASSOCIATED CONTENT

Supporting Information

FT-IR spectra and additional TEM image. This material is available free of charge via the Internet at http://pubs.acs.org.

AUTHOR INFORMATION

Corresponding Author

*E-mail: tsemrick@mail.pse.umass.edu.

Author Contributions

The manuscript was written through contributions of all authors. All authors have given approval to the final version of the manuscript.

Notes

The authors declare no competing financial interest.

ACKNOWLEDGMENTS

The authors acknowledge support for this work from the National Science Foundation (from DMR-1112455, A.L.B.; and from CHE-1152360 for the synthesis of functional conjugated polymers, T.E.). The authors also acknowledge support from the Energy Frontier Research Center at UMass Amherst, funded by the U.S. Department of Energy (DOE), Office of Science, Basic Energy Sciences (BES), under contract DE-SC0001087. Support for R.H. (morphological characterization) was provided by the DOE-BES through DE-SC0006639.

REFERENCES

(1) Li, G.; Shrotriya, V.; Huang, J.; Yao, Y.; Moriarty, T.; Emery, K.; Yang, Y. High-Efficiency Solution Processable Polymer Photovoltaic Cells by Self-Organization of Polymer Blends. *Nat. Mater.* **2005**, *4*, 864−868.

(2) Chuang, S. Y.; Chen, H. L.; Lee, W. H.; Huang, Y. C.; Su, W. F.; Jen, W. M.; Chen, C. W. Regioregularity Effects in the Chain Orientation and Optical Anisotropy of Composite Polymer/Fullerene Films for High-Efficiency, Large-Area Organic Solar Cells. *J. Mater. Chem.* **2009**, *19*, 5554−5560.

(3) Jo, J.; Na, S. I.; Lee, T. W.; Chung, Y.; Kang, S. J.; Vak, D.; Kim, K. V. Three-Dimensional Bulk Heterojunction Morphology for Achieving High Internal Quantum Efficiency in Polymer Solar Cells. *Adv. Funct. Mater.* **2009**, *19*, 2398−2406.

(4) Halls, J. M.; Walsh, C. A.; Greenham, N. C.; Marsegli, E. A.; Friend, R. H.; Moratti, S. C.; Holmes, A. B. Efficient Photodiodes From Interpenetrating Polymer Networks. *Nature* **1995**, *376*, 498−500.

(5) Peumans, P.; Uchida, S.; Forrest, S. A. Efficient Bulk Heterojunction Photovoltaic Cells using Small-Molecular-Weight Organic Thin Films. *Nature* **2003**, *45*, 158−162.

(6) Iovu, M. C.; Jeffries-El, M.; Zhang, R.; Kowalewski, T.; McCullough, R. D. Conducting Block Copolymer Nanowires Containing Regioregular Poly(3-Hexylthiophene) and Polystyrene. *J. Macromol. Chem. Part A* **2006**, *43*, 1991−2000.

(7) Rajaram, S.; Armstrong, P. B.; Kim, B. J.; Fréchet, J. M. J. Effect of Addition of a Diblock Copolymer on Blend Morphology and Performance of Poly(3-hexylthiophene):Perylene Diimide Solar Cells. *Chem. Mater.* **2009**, *21*, 1775−1777.

(8) Wienk, M. M.; Turbiez, M.; Gilot, J.; Janssen, R. A. J. Narrow-Bandgap Diketo-Pyrrolo-Pyrrole Polymer Solar Cells: The Effect of Processing on the Performance. *Adv. Mater.* **2008**, *20*, 2556−2560.

(9) Wang, C.; Kim, F. S.; Ren, G.; Xu, Y.; Pang, Y.; Jenekhe, S. A.; Jia, L. Regioregular Poly(3-alkanoylthiophene): Synthesis and Electrochemical, Photophysical, Charge Transport, and Photovoltaic Properties. *J. Polym. Sci. Part A: Polym. Chem.* **2010**, *48*, 4681−4690.

(10) Babel, A.; Jenekhe, S. A. High Electron Mobility in Ladder Polymer Field-Effect Transistors. *J. Am. Chem. Soc.* **2003**, *125*, 13656−13657.

(11) Miyakoshi, R.; Yokoyama, A.; Yokozawa, T. Development of Catalyst-Transfer Condensation Polymerization. Synthesis of π-Conjugated Polymers with Controlled Molecular Weight and Low Polydispersity. *J. Polym. Sci., Part A: Polym. Chem.* **2008**, *46*, 753−765.

(12) Zhang, Q.; Cirpan, A.; Russell, T. P.; Emrick, T. Donor−Acceptor Poly(thiophene-block-perylene diimide) Copolymers: Synthesis and Solar Cell Fabrication. *Macromolecules.* **2009**, *42*, 1079−1082.

(13) Kim, F. S.; Ren, G.; Jenekhe, S. A. One-Dimensional Nanostructures of π-Conjugated Molecular Systems: Assembly, Properties, and Applications from Photovoltaics, Sensors, and Nanophotonics to Nanoelectronics. *Chem. Mater.* **2011**, *23*, 682−732.

(14) Alivisatos, A. P. Semiconductor Clusters, Nanocrystals, and Quantum Dots. *Science* **1996**, *271*, 933−937.

(15) Ma, W. L.; Yang, C. Y.; Gong, X.; Lee, K.; Heeger, A. J. Thermally Stable, Efficient Polymer Solar Cells with Nanoscale Control of the Interpenetrating Network Morphology. *Adv. Funct. Mater.* **2005**, *15*, 1617−1622.

(16) Cui, Y.; Lieber, C. M. Functional Nanoscale Electronic Devices Assembled Using Silicon Nanowire Building Blocks. *Science* **2001**, *291*, 851−853.

(17) Xin, X.; Kim, F. S.; Jenekhe, S. A. Highly Efficient Solar Cells Based on Poly(3-butylthiophene) Nanowires. *J. Am. Chem. Soc.* **2008**, *130*, 5424−5425.

(18) Hao, X.; Reid, O. G.; Ren, G.; Kim, F. S.; Ginger, D. S.; Jenekhe, S. A. Polymer Nanowire/Fullerene Bulk Heterojunction Solar Cells: How Nanostructure Determines Photovoltaic Properties. *ACS Nano* **2010**, *4*, 1861−1872.

(19) Xin, H.; Ren, G. Q.; Kim, F. S.; Jenekhe, S. A. Bulk Heterojunction Solar Cells from Poly(3-butylthiophene)/Fullerene Blends: In Situ Self-Assembly of Nanowires, Morphology, Charge Transport, and Photovoltaic Properties. *Chem. Mater.* **2008**, *20*, 6199−6207.

(20) Moule, A. J.; Meerholz, K. Controlling Morphology in Polymer−Fullerene Mixtures. *Adv. Mater.* **2008**, *20*, 240−245.

(21) Berson, S.; Bettignies, R. D.; Bailly, S.; Guillerez, S. Poly(3-hexylthiophene) Fibers for Photovoltaic Applications. *Adv. Funct. Mater.* **2007**, *17*, 1377−1384.

(22) Park, S. H.; Yang, C.; Cowan, S.; Lee, J. K.; Wudl, F.; Lee, K.; Heeger, A. J. Isomeric Iminofullerenes as Acceptors in Bulk Heterojunction Organic Solar Cells. *J. Mater. Chem.* **2009**, *19*, 5624−5628.

(23) Lee, J. U.; Cirpan, A.; Emrick, T.; Russell, T. P.; Jo, W. H. Synthesis and Photophysical Property of Well-Defined Donor−Acceptor Diblock Copolymer Based on Regioregular Poly(3-hexylthiophene) and Fullerene. *J. Mater. Chem.* **2009**, *19*, 1483−1489.

(24) Dante, M.; Yang, C.; Walker, B.; Wudl, F.; Nguyen, T. Q. Self-Assembly and Charge-Transport Properties of a Polythiophene–Fullerene Triblock Copolymer. *Adv. Mater.* **2010**, *22*, 1835–1839.
(25) Shaw, P. E.; Ruseckas, A.; Samuel, I. D. W. Exciton Diffusion Measurements in Poly(3-hexylthiophene). *Adv. Mater.* **2008**, *20*, 3516–3520.
(26) Kim, B. J.; Miyamoto, Y.; Ma, B.; Fréchet, J. M. J. Photocrosslinkable Polythiophenes for Efficient, Thermally Stable, Organic Photovoltaics. *Adv. Funct. Mater.* **2009**, *19*, 2273–2281.
(27) Miyanishi, S.; Tajima, K.; Hashimoto, K. Morphological Stabilization of Polymer Photovoltaic Cells by Using Cross-Linkable Poly(3-(5-hexenyl)thiophene). *Macromolecules.* **2009**, *42*, 1610–1618.
(28) Page, S. M.; Martorella, M.; Parelkar, S.; Kosif, I.; Emrick, T. Disulfide Cross-Linked Phosphorylcholine Micelles for Triggered Release of Camptothecin. *Mol. Pharm.* **2013**, *10*, 2684–2692.
(29) Oku, T.; Furusho, Y.; Takata, T. A Concept for Recyclable Cross-Linked Polymers: Topologically Networked Polyrotaxane. Capable of Undergoing Reversible Assembly and Disassembly. *Angew. Chem.* **2004**, *116*, 984–987.
(30) Amamoto, Y.; Otsuka, H.; Takahara, A.; Matyjaszewski, K. Self-Healing of Covalently Cross-Linked Polymers by Reshuffl ing Thiuram Disulfide Moieties in Air under Visible Light. *Adv. Mater.* **2012**, *24*, 3975–2980.
(31) Ryu, J. H.; Chacko, R. T.; Jiwpanich, S.; Bickertan, S.; Babu, R. P.; Thayumanavan, S. Self-Cross-Linked Polymer Nanogels: A Versatile Nanoscopic Drug Delivery Platform. *J. Am. Chem. Soc.* **2010**, *132*, 17227–17235.
(32) Hammer, B. A. G.; Bokel, F. A.; Hayward, R. C.; Emrick, T. Cross-Linked Conjugated Polymer Fibrils: Robust Nanowires from Functional Polythiophene Diblock Copolymers. *Chem. Mater.* **2011**, *23*, 4250–4256.
(33) Briseno, A. L.; Mannsfeld, S. C. B.; Jenekhe, S. A.; Bao, Z.; Xia, Y. Introducing Organic Nanowire Transistors. *Mater. Today.* **2008**, 38–47.